24th INTERNATIONAL CONGRESS ON SOUND AND VIBRATION
23–27 July 2017, London

LOW ORDER MODELLING OF DIRECT AND INDIRECT COMBUSTION NOISE CONTRIBUTIONS IN A GAS TURBINE MODEL COMBUSTOR

Yasser Mahmoudi

Queen's University of Belfast, Belfast, BT9 5AH, UK
email: s.mahmoudilarimi@qub.ac.uk

Ann Dowling, Nedunchezhian Swaminathan

University of Cambridge, Cambridge, CB2 1PZ, UK

The present work deals with a low order modelling of combustion noise in a generic premixed pressurized combustor at École Centrale Paris. The exit of the combustor has choked convergent-divergent nozzle. The contributions of direct and indirect noise to the unsteady pressure within the combustor are obtained. The LOTAN (Low-Order Thermo-Acoustic Network model) code is used to obtain the Green's function for the supply ducting and combustor. LOTAN determines the linear acoustic, entropic and vortical waves due to a unit harmonic variation in the rate of heat release. We studied the effect of different upstream boundary conditions on the prediction of Green's function. To predict the combustion noise, the Green's functions are combined with the spectrum of heat release rate fluctuation. Two different ways of obtaining the power spectral density of the rate of heat release/unit volume were used; post-processing compressible LES data or using a spectral model based on the mean flow and turbulence statistics from a RANS calculation. Results show that the sound calculated using two approaches are in general in good agreement with the measured data, although the spectral method tends to under-predict the amplitude at low frequencies. It is seen that at some frequencies the indirect entropy noise is comparable to direct acoustic noise within the combustor. Previous high fidelity LES and experimental studies on this combustor have concluded that indirect entropy noise has a negligible role in the generation of the total noise in the combustor. This is because these studies could not discriminate fully between the direct and indirect noise elements: their analysis includes the multiple reflection of entropy-generated noise by the combustor boundaries as direct acoustic noise.
Keywords: combustion noise, direct and indirect noise, low order modelling

1. Introduction

The implementation of advanced low-noise aircraft engine technologies has made noise contributions from gas turbine combustors increasingly important. This is partially because advances in design have reduced the other noise sources, and partially because next generation combustion modes burn more unsteadily [1]. The broadband combustion noise radiated by a combustor comprises two components 'direct' and 'indirect'. Fluctuations in heat release from the turbulent flame generate acoustic waves which are multiply reflected from the combustor boundaries. The resulting wave pattern constitutes the 'direct' combustion noise. The 'indirect' combustion noise is generated when entropy fluctuations or vorticity perturbations are accelerated through the nozzle at the outlet of the combustor [2]. In an experiment it is very challenging to differentiate between the contributions from the direct and indirect noise in the total noise generated in the combustor. This requires development of reliable prediction tools. In this regard, the capabilities of high fidelity prediction tools based on Large Eddy Simulations (LES) and hybrid CFD/CAA-methods (computational fluid dynamics/computational

aeroacoustics) have been demonstrated to enhance the understanding of the physical processes involved in the generation of combustion noise in laboratory scale as well as full scale engines [3, 4]. Nonetheless, in addition to demanding high computational costs, these techniques are not capable of differentiating the contributions of direct and indirect combustion noise. Analytical models introduce simplifications with respect to the geometry and flow field which limit their validity to simple cases. However, more complex geometries can be represented by series of analytical elements which are linked through network models [5], the so-called 'low-order' models. These tools provide the fastest approach for the prediction of the combustion noise in the combustors under various operating conditions and are also capable of giving physical insight such as differentiating between the contributions of direct and indirect combustion noise [1, 6, 7]. To meet this requirement, the present work deals with a low order modelling of the differentiation of combustion noise sources for a generic premixed pressurized combustor (CESAM-HP combustor) at École Centrale Paris. The LOTAN (Low-Order Thermo-Acoustic Network model) code (e.g. [6-9]) is used to obtain Green's function (transfer function), which determines the linear acoustic, entropic and vortical waves due to a unit harmonic variation in the rate of heat release. To predict the combustion noise, this Green's function is combined with the spectrum of heat release rate fluctuation that is the source for combustion noise. To obtain this spectrum two approaches are utilised. For the first approach, high fidelity compressible LES data is post-processed [10]. The second approach is based on the spectral model developed by Hirsch et al. [11] and recently by Liu et al. [12]. This approach utilizes the mean and flow and turbulence quantities of a RANS to model the heat release spectrum [12]. In a recent work by Ulrich et al. [5] the LOTAN code combined with the spectral model has been shown to predict the total combustion noise in the CESAM-HP combustor. In this paper we use that solution to investigate the relative magnitudes of the direct and indirect sound.

2. CESAM-HP combustor rig

The details of the CNRS rig is given in [13] and is shown schematically in Fig. 1. The CESAM-HP test rig represents a rectangular combustion chamber with length 0.14 m, which is connected to the atmosphere via a convergent-divergent nozzle (with length of 0.219 m) mounted at the downstream end of the combustor. A straight duct with length of 0.135m and a swirler are installed upstream of the combustor to prepare premixed propane and air to inject into the combustor.

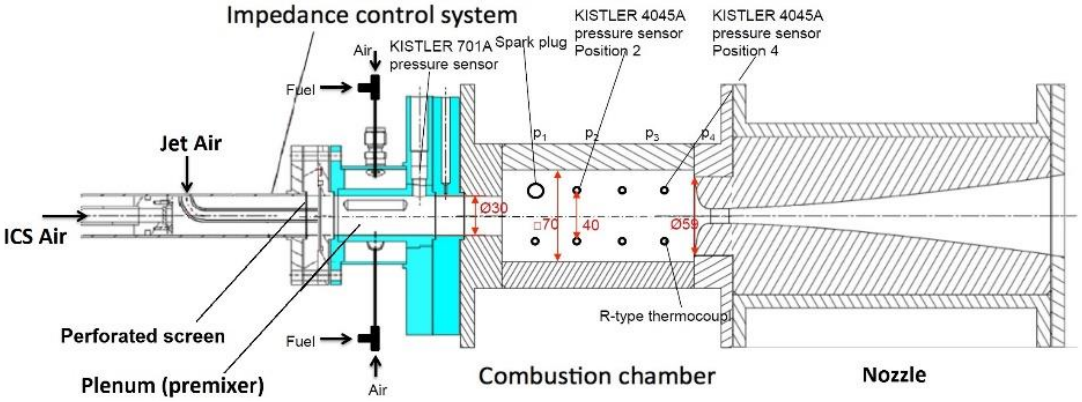

Figure 1: Schematic of CNRS combustor rig [13].

The main air enters the premixer as an axial jet injected through a perforated screen. Depending on the operating condition, additional air may be added through an Impedance Control System (ICS), which consists of a perforated plate backed by a cavity of variable depth. The ICS is used to provide an axial flow while preventing flame flashback and controlling the acoustic impedance at the inlet [13]. The supplied air flows axially through a premixing plenum where a propane-air mixture is admitted tangentially. This creates a swirling motion that increases stability during lean combustion operation and leads to a more compact flame. Then, the swirling, premixed air-propane mixture enters

the combustion chamber and is ignited by a spark plug. Thermocouples and pressure sensors are mounted at four positions within the combustor. The convergent-divergent nozzle at combustor exit accelerates the flow of burnt gases and increases the mean pressure in the combustion chamber. Indirect noise is generated in the nozzle from convected entropy fluctuations produced by the turbulent flame. The nozzle exit is open to the atmosphere.

Three different operating points were invested in the experiment are defined by different air mass flow rates through the swirler, perforated screen and axial jet inlet. The chamber was operated under lean conditions with fixed global equivalence ratio of 0.85 in each case. In the present study only one of the three operating points is investigated (referred to as OP-13-5-0) with the flow conditions given in Table 1. This operating point had the most stable combustion of the three conditions.

Table 1: Operating condition of the combustor [13] examined in this work.

Swirler mass flow	13 g/s (air) + 0.983 g/s (fuel)
Axial air of impedance control system (ICS) mass flow	0
Axial air jet mass flow	5 g/s
Equivalence ratio	0.85
Total temperature inlet	296.5 K
Mean static pressure	2.3 bar

3. Description of the model

3.1 Combustion noise spectrum

In this section we first summarise the relationship between the spectrum of heat release rate fluctuations and the spectrum of the pressure perturbations. The pressure perturbation $\hat{p}(\vec{x},\omega)$ generated by unsteady heat per unit volume can be obtained as

$$\hat{p}(\vec{x},\omega) = \int_{v_f} \hat{G}_1(\vec{y},\vec{x},\omega)\hat{q}(\vec{y},\omega)d^3\vec{y}, \tag{1}$$

where ω is the angular frequency, v_f denotes the volume of the flame brush and the circumflex denotes a perturbation from the mean. $\hat{G}_1$ is the Green's function that represents the pressure generated at $(\vec{x},\omega)$ due to a harmonic rate of heat addition at $\vec{y}$. This function is the pressure solution of linearized Euler equations in the combustor that satisfies the appropriate inlet and outlet boundary conditions. In a similar way the entropy fluctuations can be obtained as a volume integral of the product of a different Green function $\hat{G}_2$ with the rate of heat release/unit volume. We use the LOTAN network model to obtain these Green's functions $\hat{G}_1$ and $\hat{G}_2$. The power spectral density, $\hat{P}(\vec{x},\omega)$ is a statistical quantity measurable in experiments and can be calculated [12] as

$$\hat{P}(\vec{x},\omega) = \int_{v_f} \left|\hat{G}_1(\vec{y},\vec{x},\omega)\right|^2 \psi_q(\vec{y},\omega)V_{\text{cor}}\,\mathrm{d}^3\,\vec{y}. \tag{2}$$

In Eq. (2) ψ_q is the cross-power spectral density of heat release fluctuations and V_{cor} is the correlation volume of the fluctuating heat release rate whose linear dimensions are assumed to be small comparison with the acoustic and convective length scales. The Pressure Spectrum Level (PSL) in dB is hence characterized $10\log_{10}(\hat{P}/p_{ref}^2)$, where the reference acoustic pressure is $p_{ref} = 2 \times 10^{-5}$ Pa.

When the heat release is so concentrated that $\hat{G}_1(\vec{y},\vec{x},\omega)$ varies little over the combustion zone, $\hat{G}_1(\vec{y},\vec{x},\omega)$ can be taken outside the source integral with respect to source position in Eq. (2) and then LOTAN needs to be run only once for each mode number and frequency. In Eq. (2) the product of heat release rate spectrum $\psi_q(\vec{y},\omega)$ and its correlation volume needs to be integrated over the flame brush. This is equivalent to integrating the contributions from the coherent sources of combustion noise with a correlation volume V_{cor} over the flame volume. For this purpose we utilised the spectral

model of Hirsch et al. [11] modified by Liu et al. [12]. The spectrum of the heat release rate fluctuation can also be obtained using the LES simulation of the turbulent flame. We post-processed the results of compressible LES of CESAM-HP combustor [13] to predict the integral of heat release spectrum over the flame brush and the results are compared with those obtained using the spectral model.

3.2 Green's function calculation using LOTAN

The Green's function determines the linear acoustic, entropic and vortical waves due to a harmonic variation in the heat release rate. We calculate its Fourier transform $\hat{G}(\vec{y},\vec{x},\omega)$ using a network model called LOTAN (e.g. [6, 7, 9]). In LOTAN the geometry is modelled by a network of modules describing its features, such as straight ducts, area changes and heating zones. In straight duct sections, the model neglects any flow variation with radius, and assumes a uniform axial mean flow and either one- dimensional plane waves in a duct of arbitrary cross-section or circumferential modes in thin annular ducts. The network model of the CESAM-HP combustor is sketched in Fig. 2.

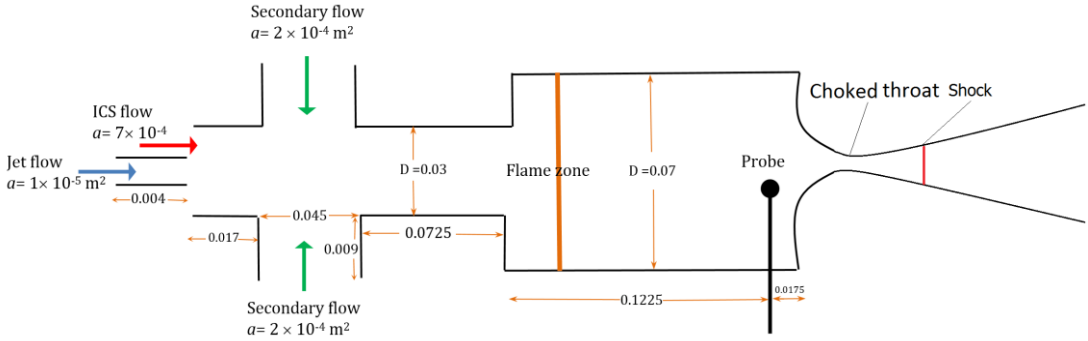

Figure 2: Schematic of CESAM-HP combustor used in LOTAN. All length dimension are in m.

For reductions in nozzle cross-sectional area and for gradual area increases, it is assumed that the mean flow does not separate so that isentropic conditions hold. Then, the mean flow quantities upstream and downstream of the area change are related to each other by applying conservation of mass, momentum and energy flow rates. The flame is modelled as a discontinuity on which the conservation of mass, momentum and energy flow rates are applied. There is a source in the energy flow rate equation due to unsteady combustion which induces frequency-dependent acoustic and entropy fluctuations. The flame is placed between 0.01m and 0.02m downstream of the inlet of the combustor and the effect of flame position on the Green's function is analysed. We assume that in the nozzle the region of supersonic flow between choked throat and the shock is compact, but the subsonic convergent and divergent sections are modelled as a series of piece-wise isentropic area changes.

The inlet of the air jet is taken to be acoustically non-reflecting. Flow in the ICS path is taken to be a short duct with length of 0.004 m. The geometry of the perforated plate such as the number of holes, holes diameter, open-area ratio and their discharge coefficients are not known. Hence, we study the effect of different boundary conditions at the ICS inlet duct considering it to be either non-reflecting or acoustically closed. As will be discussed in section 4.1 changing the boundary conditions at the inlet of the ICS duct has no noticeable effect on the pressure predicted in the combustor. The fuel-air supply is modelled as coming from a large plenum which is enters the premixing plenum tangentially through a short duct. The throat of the nozzle is choked and so the boundary condition of Marble and Candel [14] is applied at the throat. The nozzle then discharges burned gases to the atmosphere.

4. Results

In this section we first present the transfer function $\left|\hat{p}/\hat{Q}\right|$ predicted by LOTAN for total, acoustic and entropy waves at the position of fourth microphone in Fig. 1 (i.e. x = 122.5 mm from the combustor inlet). In a LOTAN calculation to obtain the direct sound, we calculate the entropy wave gen-

erated at the flame but ignore its contribution when applying the downstream choked boundary condition. The direct sound field is obtained by adding the downstream and upstream propagating acoustic waves. The indirect noise due to the entropy wave can be determined by subtracting the direct noise from the calculated full sound field. Then using the spectrum of the heat release rate fluctuation, total, direct and indirect noise generated in the combustor is predicted and compared with experimental data. It should pointed out that in the experiment and in high fidelity CFD it is very challenging to differentiate the contributions from the direct and indirect noise sources.

4.1 Effect of ICS inlet boundary condition on the transfer function (TF)

Figure 3 shows the amplitude of TF ($\left|\hat{p}/\hat{Q}\right|$) for the total noise with two different boundary conditions representing (i) Non-reflecting and (ii) Closed at the inlet of the ICS path.

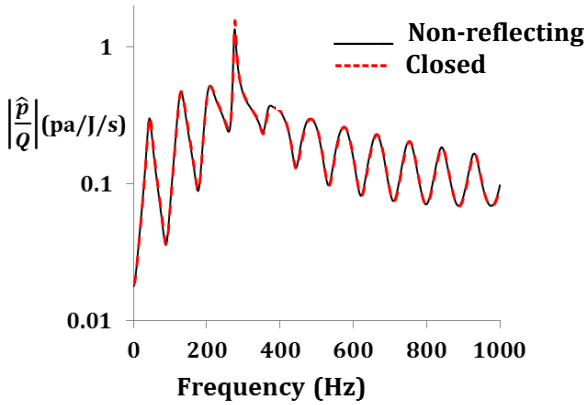

Figure 3: Amplitude of the transfer function for total noise as a function of frequency with two different boundary conditions at the inlet of the ICS, Non-reflecting (back solid line) and Closed (dashed red line).

The inlet of the jet duct is assumed to be non-reflecting and that of the fuel-air supply secondary duct is taken to be a plenum. It is seen that utilising different boundary conditions at the ICS inlet has no noticeable effect on the TF predicted in the combustor. This is because the area in the fuel-air supply secondary path is comparable to that in the main duct. Thus, its inlet plenum ensures a zero pressure perturbation and this decouples the acoustics upstream and downstream of the mixing region. Thus, in the following we set the boundary condition at the inlet of the ICS to be non-reflecting.

4.2 Effect of source position on the transfer function

When the heat release is so concentrated that $\hat{G}_1(\vec{y},\vec{x},\omega)$ varies little over the combustion zone, $\hat{G}_1(\vec{y},\vec{x},\omega)$ can be taken outside the source integral with respect to source position in Eq. (1).

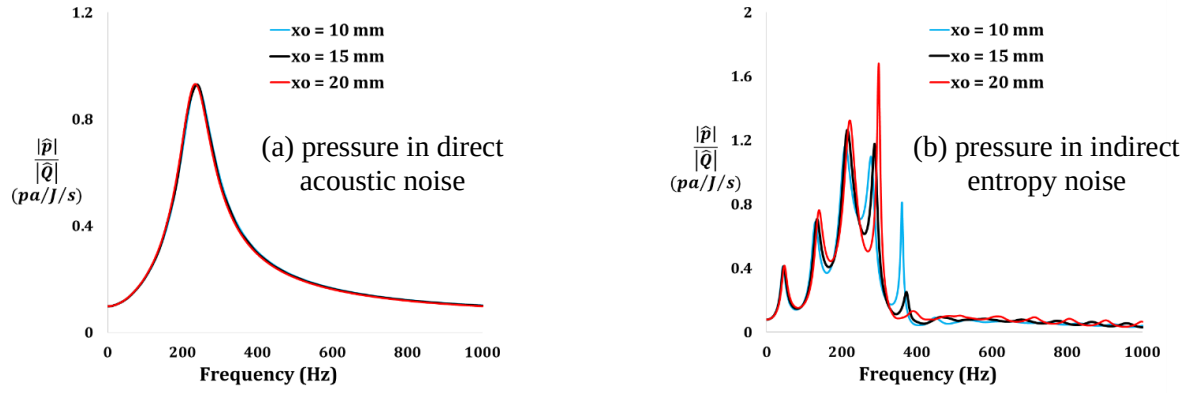

Figure 4: Amplitude of the transfer function for (a) acoustic noise and (b) entropy noise as a function of frequency with different source positions of x_o = 10 mm (blue line), x_o = 15 mm (black line) and x_o = 20 mm (red line) from inlet of the combustor.

Since the mean flow Mach number is low in the CESAM-HP combustor at the flame zone (i.e. $\bar{M}_{max} \approx 0.09$), it is a stronger constraint for the combustion zone to be short compared with the entropy wavelength $2\pi\bar{u}/\omega$ than compared with the acoustic wavelength $2\pi\bar{c}/\omega$, where $\bar{u}$ and $\bar{c}$ are the mean axial velocity and speed of sound respectively. Here the effect of source position on the Green's function has been investigated. If the Green's function is strongly dependent on $\vec{y}$, one needs to run LOTAN for a number of axial source positions. According to the RANS simulation of the CESAM-HP combustor [5], most of the heat release occurs within the first 25% of the combustor length. We consider the variation of $|\hat{G}_1|$ for a distribution of axial source positions within the first 25% of the combustor length at positions of x_o = 10, 15 and 20 mm. Transfer functions for acoustic and entropy waves are shown in Fig. 4. It is seen that the acoustic wave is not sensitive to the axial position for the range of frequencies considered. Thus, we are certain that if entropy waves are diffused before the fourth probe position, $|\hat{G}_1|$ is not sensitive to the axial source position. Indirect sound from the entropy wave shows a slight dependency on the source position mainly at the peak frequencies. However, these peaks span a very narrow-band of frequency range and hence their integral over frequency does not contribute significantly to the sound pressure level. Therefore, the results presented in Fig. 4 confirms that it is safe to take $\hat{G}_1$ outside the source integral with respect to x_o and thus LOTAN needs to be run only once for each frequency.

4.3 The transfer function of combustion noise for the combustor

Figure 5 shows the amplitude of TF of total, direct and indirect noise as a function of frequency.

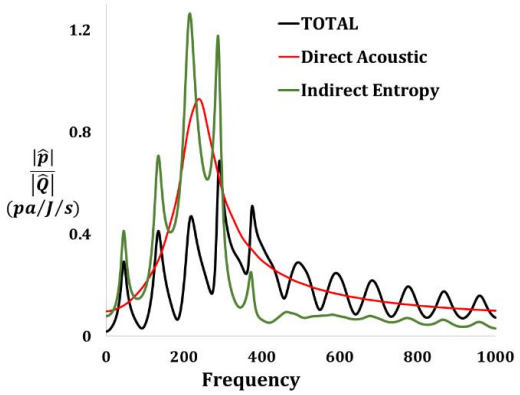

Figure 5: Amplitude of the transfer function for total (black line), direct acoustic (red line) and indirect entropy (green line) noise as a function of frequency.

It is seen that as the frequency tends to zero the TFs for total, acoustic and entropy noise tend to small values. As the frequency increase up to about f_{peak} = 250 Hz (for acoustic and entropy noise) and f_{peak} = 300Hz (for total noise) the magnitudes of the pressure increase. A further increase in the frequency leads to a decrease of the direct pressure. Entropy noise has a complicated dependence on the frequency due to it multiple resonances. The shape of the total noise is mainly affected by the entropy noise with multiple peaks and troughs. For frequencies below about 300 Hz the direct and indirect noise have similar magnitudes and contribute similarly to the total noise. For some frequencies the indirect noise is even higher than the direct noise. For higher frequencies, the contribution of the entropy noise decreases but it is still high enough to influence the total noise generated.

4.4 Sound Spectra

To predict the pressure spectrum the spectrum of the heat release rate fluctuation that is the source of direct and indirect entropy noise is obtained by two approaches, (i) by post-processing the compressible LES data of the CESAM-HP combustor [10], and (ii) using statistical noise model by Hirsch

et al. [11]. The source obtained by these approaches is multiplied by the Greens' functions as described in section 4.3. Figure 6 (a) shows the total Power Spectral Density (PSD) predicted for the combustor utilizing these two noise sources in LOTAN, and their comparison with the experimental data. It is seen that the total noise predicted by LOTAN is in good agreement with the measured data and in particular the frequency where the maximum spectral level occurs, f_{peak} = 140 Hz, is well-predicted. The Hirsch et al. [11] spectral model requires mean flow and turbulent properties such as, velocity, density, turbulent intensity, turbulent dissipation and etc which was obtained from a RANS calculation [5]. It was shown in [5] that RANS cannot predict the flow properties of the CESAM-HP combustor accurately. Consequently the there are some errors in the predicted heat release spectrum. The spectral method tends to under-predict the maximum amplitude of the integral heat release spectra and the spectral level at very low frequencies using compared to the LES data. Hence the PSD is somewhat under-predicted for low frequencies by the statistical model.

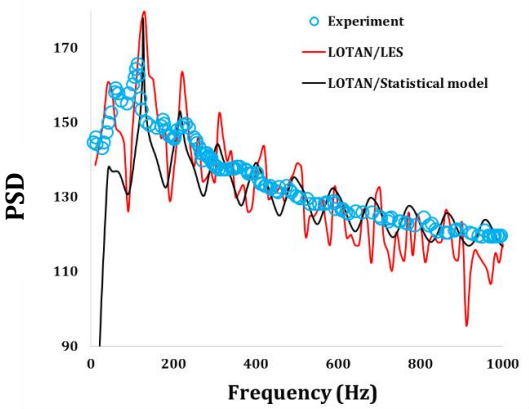

(a) PSD as a function of frequency for total predicted noise using LOTAN in combination with LES (red line), and statistical model (black line) compared with the measured data [10] (symbols).

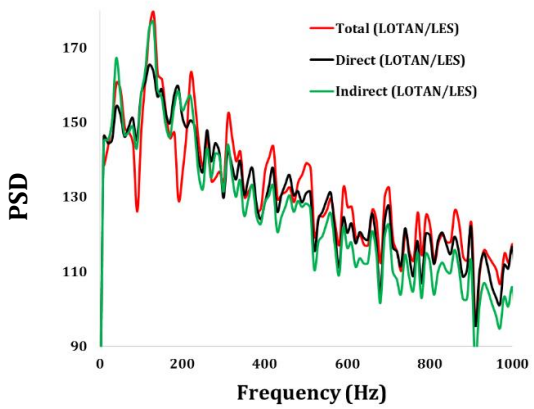

(b) PSD as a function of frequency for total noise (black line), direct acoustic (red line), indirect entropy (green line) based on heat release spectrum obtained using LES data [10].

Figure 6: Power Spectral Density (PSD) as a function of frequency.

Figure 6(b) demonstrates the contribution of direct acoustic and indirect entropy noise to the total noise generated in the CESAM-HP combustor. It is seen that the indirect entropy noise and direct acoustic noise contribute similarly to the total noise generated. Nonetheless, at frequencies above f_{peak} the contribution of the direct acoustic noise is slightly higher. Recent work by Huet et al. [10] concluded that the total noise reflected by the nozzle in the combustor is dominated by the direct contribution. This is because in their paper they discussed that their predicted direct acoustic noise includes the multiple reflection of entropy-generated noise by the combustor boundaries. Thus, in their analysis the direct and indirect noise counterparts were not fully differentiated.

5. Conclusions

A low order network model (LOTAN) has been used in combination with spectrum of the heat release rate fluctuation to predict the broadband combustion noise and its direct and indirect contributions in the laboratory-scale CESAM-HP combustor. Two approaches have been utilised to determine the spectrum of the heat release rate fluctuation for an unsteady turbulent partially premixed flame. In the first approach, results of a LES have been post-processed to calculate the spectrum of heat release rate fluctuation. In the second approach, the spectral model developed by Hirsch et al. [11] and modified by Liu et al. [12] based on RANS data, has been used to obtain an estimate of the spectrum of the heat release rate fluctuations. This heat release spectrum is then combined with the Greens' function predicted by LOTAN to obtain the spectrum of broadband pressure fluctuations due to combustion noise in the combustor. The total noise predicted utilising LES spectrum agrees well with the measured data. The statistical method tends to under-predict the measured amplitude for

frequencies below 250 Hz by up to 20 dB. But, for higher frequencies the predicted noise is in good agreement with experimental data. Contributions of direct and indirect noise sources to the total noise at the combustor outlet are identified. For frequencies below f_{peak} (the frequency of the maximum in the pressure spectrum), the indirect entropy noise makes a contribution comparable in magnitude to that of the direct acoustic noise. While for frequencies above f_{peak}, the contribution of the indirect entropy noise is modest.

6. Acknowledgements

This work was funded by the European Commission part of the RECORD (Research on Core Noise Reduction) project under Grant No. RG66913. The authors also gratefully acknowledge Wolfram Ullrich and Christoph Hirsch from TUM for making the RANS data available.

REFERENCES

1 Dowling, A. P. and Mahmoudi, Y. Combustion noise, *Proc. Combust. Inst.*, **35**, 65–100, (2015).

2 Cumpsty, N. A. Jet Engine Combustion Noise: Pressure, Entropy and Vorticity Perturbations Produced by Unsteady Combustion or Heat Addition, *J. Sound Vib.*, **66**, 527-544, (1979).

3 Kings, N., Tao, W., Scouflaire, P., Richecoeur, F., Ducruix, S. Experimental and numerical investigation of direct and indirect combustion noise contributions in a lean premixed laboratory swirled combustor, *ASME Turbo Expo 2016, American Society of Mechanical Engineers* (2016).

4 Livebardon, T., Moreau, S., Poinsot, T., Bouty, E. Numerical investigation of combustion noise generation in a full annular combustion chamber, *21th AIAA/CEAS Aeroacoustics Conference*, (2015).

5 Ulrich, W. C., Hirsch, C., Sattelmayer, T., Mahmoudi, Y., Dowling, A. P., Swaminathan, N., Lackhove, K., Sadiki, A., Fischer, A., Staufer, M. Prediction of combustion noise in a model combustor using a network and a LNSE approach, *ASME Turbo Expo 2017, American Society of Mechanical Engineers, Charlotte, United States, 26-28 June,* (Accepted), (2017).

6 Mahmoudi, Y., Dowling, A. P., Stow, S. Direct and Indirect Combustion Noise in an Idealised Combustor, *25th Int. Colloquium on the Dynamics of Explosions and Reactive Systems (ICDERS)*, Leeds, UK, (2015).

7 Mahmoudi, Y., Dowling, A. P., Stow, S. Acoustic and entropy waves in nozzles in combustion noise framework, *AIAA Journal*, (Accepted), (2017).

8 Mahmoudi, Y., Giusti, A., Mastorakos, E., Dowling, A. P. Low-order modelling of combustion noise in an aero-engine: the effect of entropy dispersion, *ASME Turbo Expo 2017, American Society of Mechanical Engineers, Charlotte, United States, 26-28 June,* (Accepted), (2017).

9 Stow, S., Dowling, A. P. A time-domain network model for nonlinear thermoacoustic oscillations, *ASME Transactions, Journal of Engineering for Gas Turbines and Power*, **131**(3), (2009).

10 Huet, M., Vuillot, F., Bertier, N., Mazur, M., Kings, N., Tao, W., Scouflaire, P., Richecoeur, F., Ducruix, S., Lapeyre, C., Poinsot, T. Recent Improvements in Combustion Noise Investigation: from the Combustion Chamber to Nozzle Flow, *AerospaceLab*, (11), 10, (2016).

11 Hirsch, C., Wasle, J., Winkler, A., Sattelmayer, T. A spectral model for the sound pressure from turbulent premixed combustion, *Proc. Combust. Inst.*, **31**, 1435–1441, (2007).

12 Liu, Y., Dowling, A. P., Swaminathan, N., Morvant, R., Macquisten, M. A., Caracciolo, L. F. Prediction of combustion noise for an aeroengine combustor, *J. Propulsion and Power*, 30(1), 114-122, (2013).

13 Mazur, M., Tao, W., Scouflaire, P., Richecoeur, F. and Ducruix, S. Experimental and Analytical Study of the Acoustic Properties of a Gas Turbine Model Combustor With a Choked Nozzle, *ASME Turbo Expo 2015, American Society of Mechanical Engineers*, (2015).

14 Marble, F.E., and Candel, S. Acoustic disturbances from gas nonuniformities convected through a nozzle, *J. Sound Vib.*, **55**, 225–243 (1977).